Journal of Power Sources 196 (2011) 683–687

Contents lists available at ScienceDirect

Journal of Power Sources

journal homepage: www.elsevier.com/locate/jpowsour

Short communication

Ionic conduction in $Sn_{1-x}Sc_xP_2O_7$ for intermediate temperature fuel cells

Hongtao Wang[a,b], Hongmin Zhang[a], Guoxian Xiao[c], Feng Zhang[d], Tian Yu[a], Jia Xiao[a], Guilin Ma[a,*]

[a] Key Laboratory of Organic Synthesis of Jiangsu Province, College of Chemistry, Chemical Engineering and Materials Science, Soochow University, Suzhou 215123, China
[b] College of Chemistry and Chemical Engineering, Fuyang Teachers College, Fuyang 236041, China
[c] Sinoma International Nanjing Cement Design & Research Institute, Nanjing 211100, China
[d] Analysis and Testing Center, Soochow University, Suzhou 215123, China

ARTICLE INFO

Article history:
Received 31 May 2010
Received in revised form 20 July 2010
Accepted 24 July 2010
Available online 3 August 2010

Keywords:
Tin pyrophosphate
Ionic conduction
Conductivity
Concentration cell
Fuel cell

ABSTRACT

A novel series of mixed ion conductors, $Sn_{1-x}Sc_xP_2O_7$ (x = 0.03, 0.06, 0.09, 0.12), were synthesized by a solid-state reaction method. The conduction behaviors of the ion conductors in wet hydrogen atmosphere were investigated by some electrochemical methods including AC impedance spectroscopy, gas concentration cells in the temperature range of 323–523 K. It was found that the doping limit of Sc^{3+} in SnP_2O_7 was between 9 mol% and 12 mol%. The highest conductivity was observed to be 2.76×10^{-2} S cm^{-1} for the sample of x = 0.06 under wet H_2 atmosphere at 473 K. The ionic conduction was contributed mainly to proton and partially to oxide ion in wet hydrogen atmosphere from 373 K to 523 K. The H_2/air fuel cells using $Sn_{1-x}Sc_xP_2O_7$ (x = 0.03, 0.06, 0.09) as electrolytes (1.7 mm in thickness) generated the maximum power densities of 11.16 mW cm^{-2} for x = 0.03, 25.02 mW cm^{-2} for x = 0.06 and 14.34 mW cm^{-2} for x = 0.09 at 423 K, respectively. The results indicated that $Sn_{1-x}Sc_xP_2O_7$ is a promising solid electrolyte system for intermediate temperature fuel cells.

1. Introduction

High temperature protonic conduction in perovskite type oxides such as doped $ACeO_3$ (A = Sr, Ba), $AZrO_3$ (A = Ca, Sr, Ba), etc. has received much attention for their potential applications in some electrochemical devices and membrane reactors [1–5]. However, high sintering and operating temperatures for these materials not only lead to metal evaporation but also bring some difficulties in choosing sealing and bonding materials. Therefore, there is a great interest in exploring new electrolyte materials with desired performances at lower sintering and operating temperatures. Considerable effort has been devoted toward the intermediate temperature fuel cells (ITFCs) based on $CsHSO_4$, CsH_2PO_4, etc. in the temperature range of 423–673 K [6,7]. Recently, numbers of tetravalent metal pyrophosphates AP_2O_7 (A = Zr, Sn, Ti, Ce, Si, etc.) were reported to have high proton conductivities [8–12]. Nagao et al. reported that the conductivities of AP_2O_7 (A = Sn, Ti, Ge, Si) increased in the order of $Ge^{4+} < Si^{4+} < Ti^{4+} < Sn^{4+}$ in unhumidified air [9], and that proton-conducting $Sn_{1-x}R_xP_2O_7$ (R = Al^{3+}, In^{3+}) were also applied to some electrochemical reactors, such as H_2/air fuel cell, selective catalytic reduction of NO_x, direct oxidation of methane to methanol, and gas sensors, etc. [13–18]. Chen et al. reported that $Sn_{0.9}In_{0.1}P_2O_7$ can conduct both protons and oxide-ions in the temperature range from 403 to 503 K [19]. Protonic conduction in $Sn_{1-x}R_xP_2O_7$ (R = Sb^{3+}, Mg^{2+}) was also reported [20,21]. Recently, we reported the protonic and oxide ionic conduction in $Sn_{1-x}Ga_xP_2O_7$ [22]. However, there is little information about ionic conduction in Sc^{3+} doped SnP_2O_7. The effective ionic radius (0.0745 nm [23]) of Sc^{3+} is close to that (0.069 nm [23]) of Sn^{4+} in 6-fold coordination. Therefore, it is interesting to investigate Sc^{3+} doped SnP_2O_7.

In this study, a novel series of intermediate temperature solid ion conductors, $Sn_{1-x}Sc_xP_2O_7$ (x = 0.03, 0.06, 0.09, 0.12), were prepared and the conduction behaviors were investigated using some electrochemical methods in the temperature range of 323–523 K. We also made estimation of the protonic and oxide ionic transport properties from the concentration cells of water vapor and hydrogen [19,24,25]. The performances of H_2/air fuel cell were tested using $Sn_{1-x}Sc_xP_2O_7$ (x = 0.03, 0.06, 0.09) as electrolytes.

2. Experimental

The initial molar ratios of phosphorus vs. metal ions, P_{ini}/(Sn + Sc), should be controlled to be 2.8 due to a fraction of phosphorus loss in the process by vaporization [13,20,22]. $Sn_{1-x}Sc_xP_2O_7$ (x = 0.03, 0.06, 0.09, 0.12) was prepared as follows. The required amounts of SnO_2 (Luoyang Ship Material Research Institute, 50–70 nm), Sc_2O_3 (99.9%) and 85% H_3PO_4 were fully mixed and held with stirring around 623 K until they became solid mixtures. The solid mixtures were ground into powder and

* Corresponding author. Tel.: +86 512 65880326; fax: +86 512 65880089.
E-mail address: 32uumagl@suda.edu.cn (G. Ma).

0378-7753/$ – see front matter © 2010 Elsevier B.V. All rights reserved.
doi:10.1016/j.jpowsour.2010.07.067

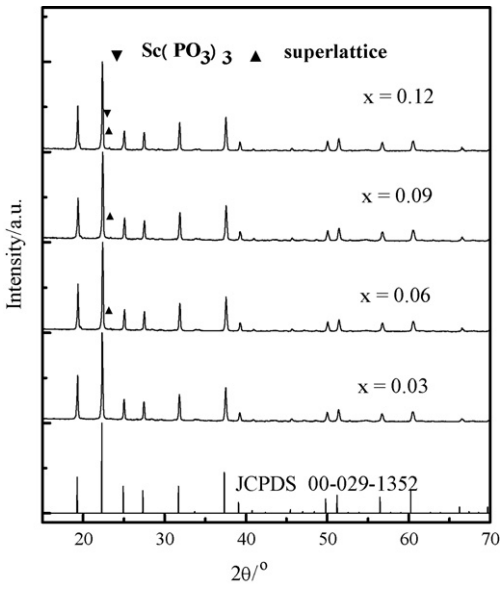

Fig. 1. XRD patterns of the $Sn_{1-x}Sc_xP_2O_7$ ($x = 0.03 - 0.12$) samples.

heat-treated at 623 K for 30 min until they became white powder, followed by sieving (100 mesh). The resulting powder was pressed into pellets at hydrostatic pressure of 300 MPa, and heat-treated at 873 K for 2 h to obtain $Sn_{1-x}Sc_xP_2O_7$ samples. The crystalline structure of the $Sn_{1-x}Sc_xP_2O_7$ samples was determined at room temperature by X-ray diffraction (XRD) analysis. The microstructures of the samples were observed by a scanning electron microscope (SEM). Platinum paste was coated on both sides (area: 0.5 cm^2) of the heat-treated pellets (diameter 20 mm, thickness 1.4–1.8 mm) and heated at 523 K for 30 min. The pellets were connected to Pt wires and sealed between two alumina tubes, and then placed into an electric furnace for electrochemical measurements. The conductivities were measured in wet H_2 atmosphere at 323–523 K by an AC impedance method using electrochemical workstations (Zahner IM6ex). The frequency range for the measurements was 1 Hz to 3 MHz and the ac amplitude was 10 mV. Wet gases were obtained by saturating water vapor at 298 K.

In order to study the ionic conduction in the samples, hydrogen and water vapor concentration cells were constructed and the electromotive forces (EMFs) were measured at 373–523 K. The H_2/air fuel cell using $Sn_{1-x}Sc_xP_2O_7$ ($x = 0.03$, 0.06, 0.09) as electrolytes and porous platinum as cathode and anode was constructed. The current–voltage curves were measured to evaluate the performance of the fuel cell.

3. Results and discussion

3.1. X-ray diffraction

The structure of SnP_2O_7-based compounds is very complicated. A pseudo-cubic $3 \times 3 \times 3$ superlattice was observed at room temperature in SnP_2O_7 by electron diffraction [26]. After heat-treated at 873 K for 2 h, some weak peaks, which cannot be indexed by the cubic structure appeared, but may be indexed by the orthorhombic superlattice, were observed in $Sn_{0.9}In_{0.1}(P_2O_7)_{1-\delta}$ prepared by aqueous solution method [10]. Fig. 1 shows the powder X-ray diffraction (XRD) patterns of $Sn_{1-x}Sc_xP_2O_7$ samples with various Sc^{3+} doping levels. It can be seen from Fig. 1 that the sample of $x = 0.03$ shows a single cubic phase structure in agreement with that of SnP_2O_7 in JCPDS (00-029-1352), while the samples of $x \geq 0.06$ show a weak peak at $2\theta \approx 23^\circ$, which cannot be indexed by the cubic structure, probably due to the formation of the pseudo-cubic $3 \times 3 \times 3$ superlattice [10]. The lattice parameters for the samples of $x = 0.03$, 0.06, 0.09, 0.12 were calculated to be a = 0.7941(5) nm, 0.7939(5) nm, 0.7942(4) nm and 0.7935(5) nm, correspondingly. The effective ionic radius (0.0745 nm [23]) of Sc^{3+} is larger than that (0.069 nm [23]) of Sn^{4+} in 6-fold coordination. Therefore, the lattice parameter is expected to increase with increasing doping level. The sample of $x = 0.09$ shows the maximum lattice parameter, whereas the sample of $x = 0.12$ shows the smallest lattice parameter among the determined samples. The significant decrease in lattice parameter of $x = 0.12$ sample is likely due to the loss of larger scandium in the pyrophosphate phase with the formation of $Sc(PO_3)_3$ [10]. This may be also confirmed by comparing the intensities of weak peaks at $2\theta \approx 23^\circ$ of the samples. A weak peak of $Sc(PO_3)_3$ is at $2\theta \approx 23^\circ$, which is the same position as that of the weak peak of the pseudo-cubic $3 \times 3 \times 3$ superlattice. For the samples of $x = 0.06$ and 0.09, the weak peaks at $2\theta \approx 23^\circ$ have almost same intensities, implying the formation of the pseudo-cubic $3 \times 3 \times 3$ superlattice. However, for the samples of $x = 0.12$, the weak peak at $2\theta \approx 23^\circ$ has larger intensity. This may be also a proof of the appearance of $Sc(PO_3)_3$ impurity in the $x = 0.12$ sample. From the above results, it may be believed that the solid solution limit in $Sn_{1-x}Sc_xP_2O_7$ was at least $x = 0.09$.

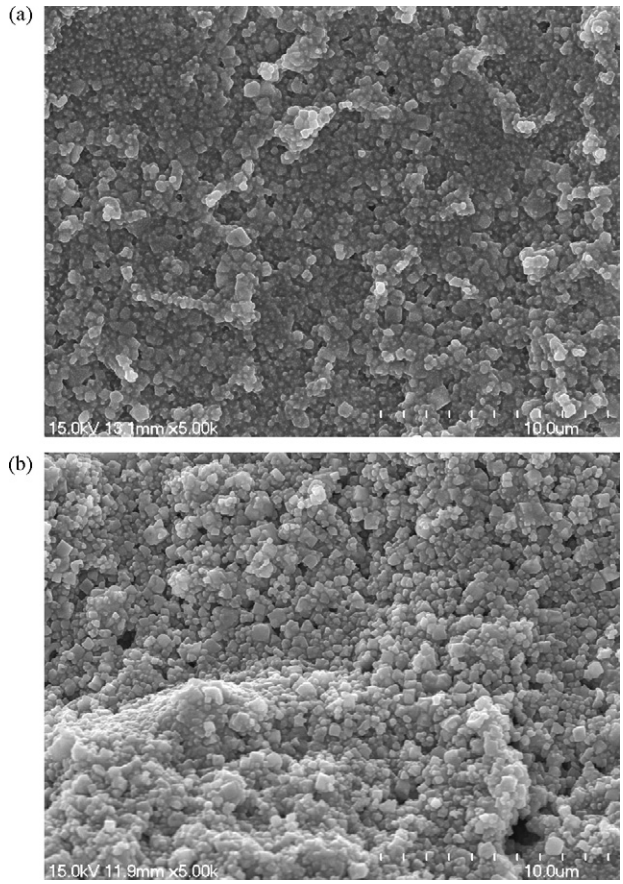

Fig. 2. SEM images of external surface of (a) $x = 0.06$ and (b) $x = 0.12$ pellet samples heat-treated at 873 K for 2 h.

3.2. SEM image

Typical SEM images of external surface of $x = 0.06$ and 0.12 pellet samples heat-treated at 873 K for 2 h are displayed in Fig. 2. As seen from Fig. 2, the primary particles have sphere-like shapes, and the particle size distributions are about 200–600 nm in diameter. This is similar to the observation for Al^{3+}-doped SnP_2O_7 prepared through

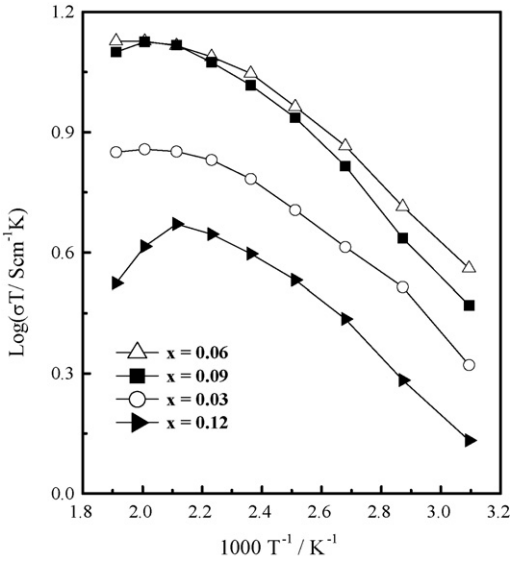

Fig. 3. Temperature dependence of electrical conductivity of $Sn_{1-x}Sc_xP_2O_7$ ($x = 0.03$, 0.06, 0.09, 0.12) in wet H_2 atmosphere at 323–523 K.

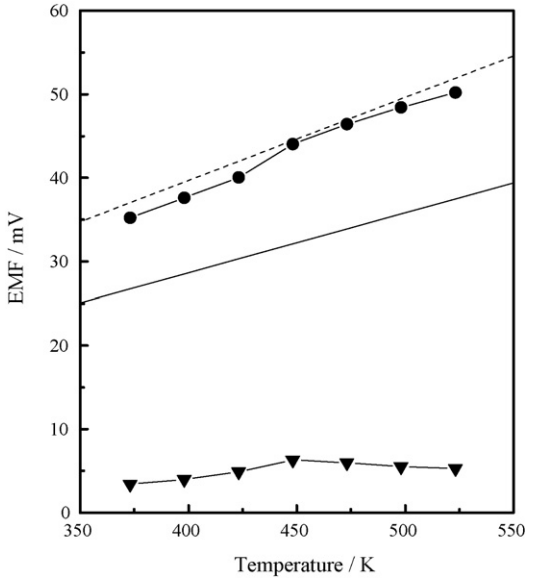

Fig. 4. EMFs of the hydrogen concentration cell: H_2, Pt $|Sn_{1-x}Sc_xP_2O_7$ ($x = 0.06$)| Pt, H_2–Ar ($p_{H_2} = 1.01 \times 10^4$ Pa) and EMFs of the water vapor concentration cell: H_2 ($p_{H_2O} = 2.34 \times 10^3$ Pa), Pt| $Sn_{1-x}Sc_xP_2O_7$ ($x = 0.06$)| Pt, H_2 ($p_{H_2O} = 1.23 \times 10^4$ Pa). The operating temperatures are from 373 K to 523 K. Dotted line indicates the theoretical value and symbol ● represents the observed value of EMF of the hydrogen concentration cell at each temperature. Solid line indicates the theoretical value and symbol ▼represents the observed value of EMF of the water vapor concentration cell at each temperature.

similar heat treatments [13]. It may be seen also from Fig. 2 that some pores occur in pellet samples, which may result in decrease of the densities of the pellet samples and physical leakage of gas through the samples [9]. The relative densities of the pellet samples prepared in this study were estimated to be 70–80%, which are much lower than traditional ceramics, e.g. YSZ, doped CeO_2, etc. In order to enhance electrical conduction and application performances, it is necessary to increase relative density of Sc-doped SnP_2O_7 through adopting more effective preparation methods.

3.3. Effect of Sc^{3+} doping level on the conductivities

Fig. 3 shows Arrhenius plots of the total conductivities of the samples in wet H_2 atmosphere from 323 K to 523 K. It is clear that the conductivities increased in the order: σ ($x = 0.12$) < σ ($x = 0.03$) < σ ($x = 0.09$) < σ ($x = 0.06$). The influence of the doping level of Sc^{3+} at Sn^{4+} sites on the conductivities may be attributed to the effective concentration of oxygen vacancy and impurity phase of $Sc(PO_3)_3$. The higher Sc^{3+} doping level resulted in the higher oxygen vacancy concentration, nevertheless, the concentrations of point defect pairs, $Sc'_{Sn}V_O^{\bullet\bullet}$, $Sc'_{Sn}V_O^{\bullet\bullet}Sc'_{Sn}$, and $Sc'_{Sn}OH_O^{\bullet}$, also increase at the same time. Considering the opposite two factors above, the effective concentrations of oxygen vacancy may reach its maximum value at $x = 0.06$ [22]. As a result, the highest conductivity 2.76×10^{-2} S cm^{-1} was observed for the sample of $x = 0.06$ under a wet H_2 atmosphere at 473 K. The conductivities of samples of $x > 0.06$ decreased with the increasing doping levels due to the formation of the secondary $Sc(PO_3)_3$ phase and lower effective oxygen vacancy concentrations. The effect of the formation of the pseudo-cubic $3 \times 3 \times 3$ superlattice on the conductivities is still unclear in present stage.

3.4. Concentration cell measurements

For a concentration cell containing hydrogen and water vapor, the observed values (EMF_{obs}) of electromotive forces are given by following Nernst equation [19,24,25].

$$EMF_{obs} = \frac{RT}{2F}\left\{-t_{ion}\ln\left[\frac{p_{H_2(II)}}{p_{H_2(I)}}\right] + t_O \ln\left[\frac{p_{H_2O(II)}}{p_{H_2O(I)}}\right]\right\}$$

If the p_{H_2} in both cell compartments is the same, i.e. $p_{H_2(II)} = p_{H_2(I)}$, the EMF of water vapor concentration cell gives the transference numbers of oxide-ions (t_O). Similarly, the EMF of hydrogen concentration cell with $p_{H_2O(II)} = p_{H_2O(I)}$ gives the ionic contribution. The ionic transport number t_{ion} ($= t_H + t_O$) can be obtained by EMF_{obs}/EMF_{cal}, where $EMF_{cal} = RT/2F \ \ln[p_{H_2(II)}/p_{H_2(I)}]$. Electronic transport number t_e can be given to $t_e = 1 - (t_H + t_O)$.

Typical results using sample of $x = 0.06$ as an electrolyte of gas concentration cells are shown in Fig. 4. In Fig. 4, pure hydrogen and a mixture of H_2–Ar ($p_{H_2} = 1.01 \times 10^4$ Pa) are applied as the electrode gases. The electrode with higher pressure of hydrogen gas is negative [27]. Dotted line indicates the theoretical value and symbol ● represents the observed EMF value of the hydrogen concentration cell at each temperature. Obviously, each observed EMF value of hydrogen concentration cell is close to the corresponding theoretical one. The ionic transport number t_{ion} is almost unity with value of 0.95–0.99, the rest is electronic transport number ($t_e = 0.01$–0.05) in wet hydrogen atmosphere at 373–523 K. Therefore, the total conductivities of the samples in wet hydrogen atmosphere shown in Fig. 3 is almost pure ionic.

The oxide ionic transport number (t_O) in wet hydrogen atmosphere may also be evaluated from water vapor concentration cell shown in Fig. 4. Solid line indicates the theoretical value and symbol ▼represents the observed EMF value of the water vapor concentration cell at each temperature. The t_O is calculated to be 0.13–0.20 at 373–523 K, indicating the existence of oxide ionic conduction under low oxygen partial pressure condition. Thus, the protonic transport number ($t_H = t_{ion} - t_O$) is calculated to be 0.79–0.82. In wet hydrogen atmosphere, protonic conduction appears due to defect reactions (1) and (2) [9], resulting in the prevailing protonic conduction in wet hydrogen atmosphere [22].

$$H_2O\,(g) + V_O^{\bullet\bullet} + O_O^{\times} \Leftrightarrow 2OH_O^{\bullet} \quad (1)$$

$$H_2O\,(g) + 2h^{\bullet} + 2O_O^{\times} \Leftrightarrow 2OH_O^{\bullet} + 1/2O_2 \quad (2)$$

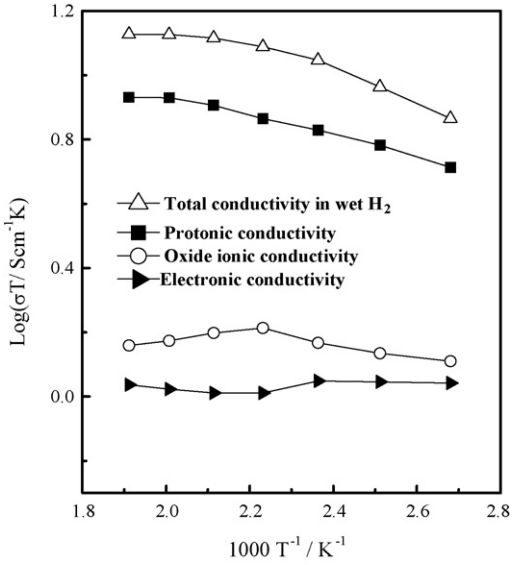

Fig. 5. Partial conductivities of charged species in wet hydrogen atmosphere. The operating temperatures are from 373 K to 523 K.

3.5. Partial conductivities of charged species

In wet hydrogen atmosphere, the total conductivity $\sigma_t = \sigma_H + \sigma_o + \sigma_e$. The protonic, oxide ionic and electronic conductivities are calculated from $\sigma_H = \sigma_t \times t_H$, $\sigma_O = \sigma_t \times t_O$ and $\sigma_e = \sigma_t \times t_e$, respectively. The results are shown in Fig. 5. It is clear from Fig. 5 that the total conductivity ($\sigma_t = 1.96 \times 10^{-2}$–$2.76 \times 10^{-2}$ S cm^{-1}) is one to two orders of magnitude higher than the electronic conductivity ($\sigma_e = 2.74 \times 10^{-4}$–$1.21 \times 10^{-3}$ S cm^{-1}). The maximum protonic conductivity is observed to be 2.24×10^{-2} S cm^{-1} at 473 K, which is higher than that in $BaCe_{0.85}Y_{0.15}O_{3-\alpha}$ (1.04×10^{-2} S cm^{-1}) under wet hydrogen atmosphere at 873 K [28]. The relatively low electronic conductivity in wet hydrogen atmosphere confirmed that this material is a good ionic conductor [9,22].

3.6. Performance of H_2/air fuel cell

Fig. 6 shows the current–voltage–power (*I–V–P*) curves of the H_2/air fuel cells: wet H_2 ($p_{H_2O} = 3.2 \times 10^3$ Pa), Pt|$Sn_{1-x}Sc_xP_2O_7$ (x = 0.03, 0.06, 0.09)|Pt, wet Air ($p_{H_2O} = 3.2 \times 10^3$ Pa). The operating temperature is 423 K, the thickness of electrolytes is 1.7 mm and the flow rates of H_2 and air gases are all 30 ml min^{-1} during the experiment. The theoretical electromotive force value (EMF) may be calculated according to literature method [22]. As shown in Fig. 6, the open circuit voltages are around 0.97 V, which are lower than the theoretical one (1.216 V at 423 K). The difference may be relevant to the electronic conduction in the samples as shown in Figs. 4 and 5, and relevant to some physical leakage of gas through the electrolyte due to lower relative density of the electrolyte. It can be seen from Fig. 6 that the peak power densities of the cells reached 11.16 mW cm^{-2} for x = 0.03, 25.02 mW cm^{-2} for x = 0.06 and 14.34 mW cm^{-2} for x = 0.09 sample, correspondingly, which is similar to the data reported by Chen et al. for $Sn_{0.9}In_{0.1}P_2O_7$ [19]. The cell performance may be enhanced by doping suitable ions and levels. The results indicated that $Sn_{1-x}Sc_xP_2O_7$ is a promising solid electrolyte system for intermediate temperature fuel cells.

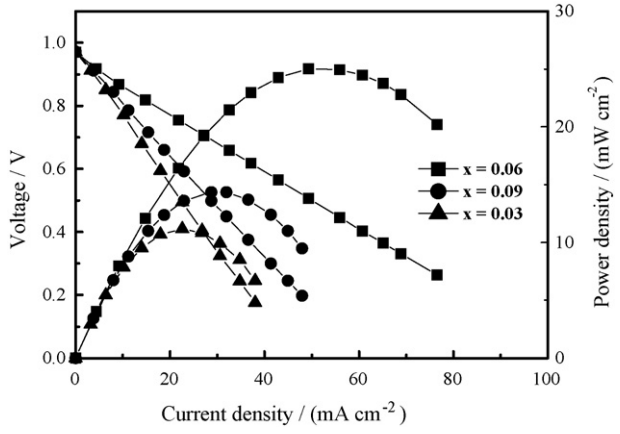

Fig. 6. *I–V–P* curves for a hydrogen/air fuel cell using $Sn_{1-x}Sc_xP_2O_7$ (x = 0.03, 0.06, 0.09) as electrolytes at 423 K. Electrolyte thickness: 1.7 mm.

4. Conclusions

In this study, a novel series of samples $Sn_{1-x}Sc_xP_2O_7$ (x = 0.03, 0.06, 0.09, 0.12, 0.15) were prepared. The doping limit of Sc^{3+} in SnP_2O_7 was at least x = 0.09. It was found that the conductivities increased with various Sc^{3+} doping levels in the order: σ (x = 0.12) < σ (x = 0.03) < σ (x = 0.09) < σ (x = 0.06). The highest conductivity was observed to be 2.76×10^{-2} S cm^{-1} for the sample of x = 0.06 under wet H_2 atmosphere at 473 K. The ionic transport numbers (t_{ion} = 0.95–0.99) are close to unity, and the relatively low electronic conductivity in wet hydrogen atmosphere indicated that this material is a good ionic conductor. The maximum proton conductivity (2.24×10^{-2} S cm^{-1}) at 473 K is higher than that in $BaCe_{0.85}Y_{0.15}O_{3-\alpha}$ (1.04×10^{-2} S cm^{-1}) under wet hydrogen atmosphere at 873 K. The H_2/air fuel cells using $Sn_{1-x}Sc_xP_2O_7$ (x = 0.03, 0.06, 0.09) as electrolytes (thickness: 1.7 mm) generated the maximum power densities of 11.16 mW cm^{-2} for x = 0.03, 25.02 mW cm^{-2} for x = 0.06 and 14.34 mW cm^{-2} for x = 0.09 at 423 K, respectively. $Sn_{1-x}Sc_xP_2O_7$ may be a promising solid electrolyte system for intermediate temperature fuel cells.

Acknowledgements

This work was supported by the National Natural Science Foundation of China (No. 20771079), Soochow University subsidizing project (No. KY2010063A), Anhui province subsidizing project (No. 2008Z038).

References

[1] X.-Z. Fu, J.-L. Luo, A.R. Sanger, N. Luo, K.T. Chuang, J. Power Sources 195 (2010) 2659.
[2] P. Pasierb, M. Wierzbicka, S. Komornicki, M. Rekas, J. Power Sources 194 (2009) 31.
[3] Y.-M. Kim, P.K-. Lohsoontorn, J. Bae, J. Power Sources 195 (2010) 6420.
[4] H. Iwahara, Y. Asakura, K. Katahira, M. Tanaka, Solid State Ionics 168 (2004) 299.
[5] R.T. Baker, R. Salar, A.R. Potter, I.S. Metcalfe, M. Sahibzada, J. Power Sources 191 (2009) 448.
[6] S.M. Haile, D.A. Boysen, C.R.I. Chisholm, R.B. Merle, Nature 410 (2001) 910.
[7] D.A. Boysen, T. Uda, C.R.I. Chisholm, S.M. Haile, Science 303 (2004) 68.
[8] S. Teranishi, K. Kondo, M. Nishida, W. Kanematsu, T. Hibino, Electrochem. Solid-State Lett. 12 (2009) J73.
[9] M. Nagao, T. Kamiya, P. Heo, A. Tomita, T. Hibino, M. Sano, J. Electrochem. Soc. 153 (2006) A1604.
[10] S. Tao, Solid State Ionics 180 (2009) 148.
[11] V. Nalini, R. Haugsrud, T. Norby, Solid State Ionics 181 (2010) 510.
[12] X. Sun, S. Wang, Z. Wang, X. Ye, T. Wen, F. Huang, Solid State Ionics 179 (2008) 1138.
[13] A. Tomita, N. Kajiyama, T. Kamiya, M. Nagao, T. Hibino, J. Electrochem. Soc. 154 (2007) B1265.
[14] M. Nagao, A. Takeuchi, P. Heo, T. Hibino, M. Sano, A. Tomita, Electrochem. Solid-State Lett. 9 (2006) A105.
[15] A. Tomita, T. Yoshii, S. Teranishi, M. Nagao, T. Hibino, J. Catal. 247 (2007) 137.
[16] A. Tomita, J. Nakajima, T. Hibino, Angew. Chem. Int. Ed. 47 (2008) 1462.
[17] S. Teranishi, K. Kondo, A. Tsuge, T. Hibino, Sens. Actuators B 140 (2009) 170.
[18] Y. Jin, B. Lee, T. Hibino, J. Jpn. Petrol. Inst. 53 (2010) 12.

[19] X. Chen, C. Wang, E.A. Payzant, C. Xia, D. Chu, J. Electrochem. Soc. 155 (2008) B1264.
[20] X. Wu, A. Verma, K. Scott, Fuel Cells 8 (2008) 453.
[21] K. Genzaki, P. Heo, M. Sano, T. Hibino, J. Electrochem. Soc. 156 (2009) B806.
[22] H. Wang, J. Liu, W. Wang, G. Ma, J. Power Sources 195 (2010) 5596.
[23] R.D. Shannon, Acta Cryst. A32 (1976) 751.
[24] T. Shimada, C. Wen, N. Taniguchi, J. Otomo, H. Takahashi, J. Power Sources 131 (2004) 289.
[25] T. Shimura, K. Esaka, H. Matsumoto, H. Iwahara, Solid State Ionics 149 (2002) 237.
[26] R.K.B. Gover, N.D. Withers, S. Allen, R.L. Withers, J.S.O. Evans, J. Solid State Chem. 166 (2002) 42.
[27] G.L. Ma, F. Zhang, J.L. Zhu, G.Y. Meng, Chem. Mater. 18 (2006) 6006.
[28] Y.X. Guo, B.X. Liu, C. Chen, W.B. Wang, G.L. Ma, Electrochem. Commun. 11 (2009) 153.